Virology **255,** 260–268 (1999)
Article ID viro.1998.9554, available online at http://www.idealibrary.com on IDEAL®

Flexibility of the Major Antigenic Loop of Foot-and-Mouth Disease Virus Bound to a Fab Fragment of a Neutralising Antibody: Structure and Neutralisation

Nuria Verdaguer,* Guy Schoehn,† Wendy F. Ochoa,* Ignacio Fita,* Sharon Brookes,‡ Andrew King,‡ Esteban Domingo,§ Mauricio G. Mateu,§ David Stuart,¶,‖ and Elizabeth A. Hewatt†,[1]

*Departamento de Biología Molecular y Celular, CID (CSIC), Jordi Girona 18-26, 08034 Barcelona, Spain; †Institut de Biologie Structurale Jean-Pierre Ebel (CEA, CNRS), 41 Av. des Martyrs, 38027 Grenoble, France; ‡Institute for Animal Health, Pirbright Laboratory, Ash Road, Pirbright, Woking GU24 0NF, United Kingdom; §Centro de Biología Molecular "Severo Ochoa" (CSIC-UAM), Universidad Autonoma de Madrid, 28049 Madrid, Spain; ¶Laboratory of Molecular Biophysics, University of Oxford, South Parks Road, Oxford, OX1 3QU, United Kingdom; and ‖Oxford Centre for Molecular Sciences, University of Oxford, South Parks Road, Oxford, OX1 3QT, United Kingdom

Received October 2, 1998; returned to author for revision November 9, 1998; accepted November 30, 1998

The interaction of foot-and-mouth disease virus (FMDV) serotype C (clone C-S8c1) with a strongly neutralising monoclonal antibody (MAb) 4C4 has been studied by combining data from cryoelectron microscopy and x-ray crystallography. The MAb 4C4 binds to the exposed flexible GH-loop of viral protein 1 (VP1), which appears to retain its flexibility, allowing movement of the bound Fab. This is in striking contrast to MAb SD6, which binds to the same GH-loop of VP1 but exhibits no movement of the bound Fab when observed under identical conditions. However, MAbs 4C4 and SD6 have very similar neutralisation characteristics. The known atomic structure of FMDV C-S8c1 and that of the 4C4 Fab cocrystallised with a synthetic peptide corresponding to the GH-loop of VP1 were fitted to the cryoelectron microscope density map. The best fit of the 4C4 Fab is compatible only with monovalent binding of the MAb in agreement with the neutralisation data on 4C4 MAbs, Fab2s, and Fabs. The position of the bound GH-loop is related to other known positions of this loop by a hinge rotation about the base of the loop. The 4C4 Fab appears to interact almost exclusively with the G-H loop of VP1, making no other contacts with the viral capsid.

INTRODUCTION

Foot-and-mouth disease virus (FMDV) is an important animal pathogen of the genus Aphthovirus of the family Picornaviridae (Rueckert, 1996). The virus is genetically and antigenically variable (Domingo *et al.,* 1992), and this presents one of the main problems in the design of effective synthetic vaccines (Taboga *et al.,* 1992). Neutralising antibodies appear as major determinants of protection against FMDV infection (Mateu, 1995; McCullough *et al.,* 1992). Structural and functional studies have documented that the G-H loop of capsid protein VP1 of FMDV has a dual function. It includes an Arg-Gly-Asp (RGD) triplet involved in recognition of integrin $\alpha_v\beta_3$, one of the receptors for FMDV (Berinstein *et al.,* 1995; Fox *et al.,* 1989; Hernandez *et al.,* 1996; Jackson *et al.,* 1997; Mason *et al.,* 1994; Sharma *et al.,* 1997). In addition, the same G-H loop contains a major antigenic determinant, and synthetic peptides consisting of amino acid sequences of the loop are able to induce neutralising antibodies in animals (Bittle *et al.,* 1982; Di Marchi *et al.,* 1986; Pfaff *et al.,* 1982). This antigenic loop protrudes from the relatively smooth surface of FMD virions, and it appears to be mobile as judged by the lack of well-defined electronic density in crystals of FMDV particles (Acharya *et al.,* 1989; Curry *et al.,* 1996; Lea *et al.,* 1994, 1995). A structure of the loop could be determined on chemical reduction of FMDV O_1 BFS particles (Logan *et al.,* 1993).

For FMDV of serotype C (clone C-S8c1) (Sobrino *et al.,* 1983), this major antigenic site, termed site A, has been studied in detail by examining neutralisation escape mutants and by measuring the reactivity of antibodies with synthetic peptides bearing specific amino acid substitutions. These studies show that antigenic site A is composed of several distinct, overlapping, continuous epitopes located between residues 136 and 150 of VP1 (Mateu, 1995; Mateu *et al.,* 1989, 1990). The three-dimensional structures of the Fab fragment of two neutralising monoclonal antibodies (MAbs) raised against FMDV type C, complexed with an antigenic peptide representing site A, have been determined (Verdaguer *et al.,* 1995, 1996, 1998). Interestingly, even though these two MAbs (SD6 and 4C4, described in Mateu *et al.* (1990) recognise two different epitopes within site A, the antigenic peptide adopts a very similar quasicircular structure in both complexes (Verdaguer *et al.,* 1998). This structure, in which the RGD triplet forms an open-turn flanked by a β-strand and a helical region, is similar to the structure of the loop

[1] To whom reprint requests should be addressed. Fax: 33-0-476-885494. E-mail: hewat@lmes.ibs.fr.

0042-6822/99 $30.00

in the reduced FMDV O_1 BFS (Logan *et al.,* 1993). In the two antigen-Fab structures analysed, the Asp143, which is critical for integrin-recognition function, also establishes major interactions with residues of the variable regions of the antibodies (Verdaguer *et al.,* 1995, 1998). Moreover, the analysis of reactivity of additional site A-specific, neutralising antibodies with substituted synthetic peptides indicates that in all cases Asp143 and some adjacent residues play an essential role in antibody recognition (Verdaguer *et al.,* 1998).

Cryoelectron microscopy data on the Fab SD6 complexed to FMDV C-S8c1 particles, combined with information from x-ray crystallography of a complex of the Fab with the peptide antigen, allowed the positioning of the antigenic loop on the virion surface (Hewat *et al.,* 1997). The loop is bent toward the fivefold axis, near the B-C loop of VP1, similar to the "up" position proposed for native FMDV of serotype O (Parry *et al.,* 1990). This orientation is opposed to the "down" position observed for the loop in chemically reduced FMDV O particles (Logan *et al.,* 1993). The Fab SD6 projects almost radially from the viral surface in an orientation that was compatible only with monovalent attachment of the antibody. This was also supported by studies on neutralisation of infectivity with MAb SD6 (Verdaguer *et al.,* 1997). The results suggest that neutralisation by MAb SD6 involves blocking the receptor-recognition site through monovalent binding. The picture emerging from these studies is that antigenic site A of FMDV exists as a defined quasicircular shape that tolerates little structural perturbations but that may be subjected to hinge movements on the virion surface (Logan *et al.,* 1993; Parry *et al.,* 1990; Verdaguer *et al.,* 1998). The possible implication of loop movements for the immunogenicity or antigenicity of FMDV is a critical question for which no information is available. In the present report, we analyse the cryoelectron microscopic binding of the Fab 4C4 to FMDV C-S8c1 and compare the neutralisation of the virus by the entire MAb and their Fab and Fab2 moieties. The structural analyses provide evidence of flexibility of the Fab bound to a fully exposed G-H loop that occupies positions distinct from those previously identified in FMDV C-S8c1 complexed to MAb SD6 or in reduced type O FMDV. The results reinforce monovalent antibody binding as the mechanism of FMDV neutralisation by this group of antibodies.

RESULTS AND DISCUSSION

Cryoelectron microscopy of FMDV C-S8c1/4C4-Fab complexes

Cryoelectron microscopy images of frozen hydrated complexes between FMDV C-S8c1 and 4C4-Fab revealed that all the 300-Å-diameter virions were decorated with Fabs (Fig. 1). However, the fringe of Fabs projecting from the virions appeared heterogeneous, thus indicating a partial occupancy and/or flexibility of the bound Fabs. Images of the complex between FMDV C-S8c1 and the SD6-Fab obtained under practically identical conditions showed a much more homogeneous decoration of Fabs projecting radially from the virion surface (Hewat *et al.,* 1997). No empty capsids, decorated or not, were observed.

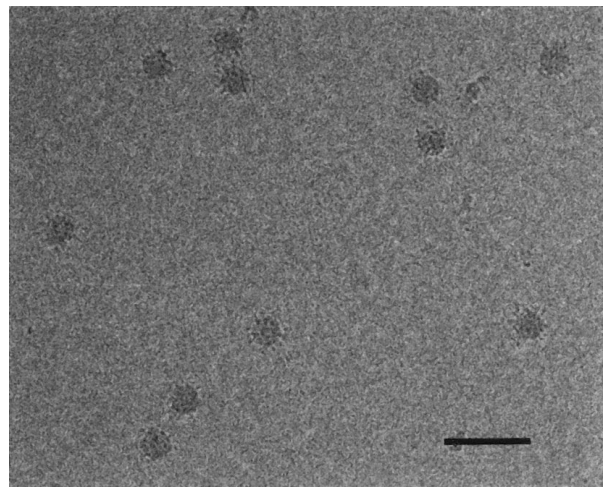

FIG. 1. Electron micrograph of frozen hydrated FMDV C-S8c1/4C4-Fab at a defocus of ~1.8 μm. The scale bar represents 1000 Å.

Reconstructed density of the FMDV C-S8c1/4C4-Fab complex

Isosurface representations of the FMDV C-S8c1/4C4-Fab complex show the nearly spherical FMDV C-S8c1 decorated with 60 Fabs that project from the surface at an angle of ~20 to 25 degrees to the normal to the capsid surface (Fig. 2). In the reconstruction, the maximum density corresponding to the 4C4 Fab is lower than that in the viral capsid (50–60%), but it spans a volume roughly twice as large as that of a single Fab. The relatively poorly defined, smeared-out shape of the Fab density is consistent with a flexibility of the bound Fab about the binding site (Fig. 3). Determination of the occupancy is not straightforward when movement is involved as well. We suppose that the occupancy is quite high, partly because of the large volume of density for the Fab and partly because the neutralisation experiments suggest a high affinity of MAb 4C4 for FMDV C-S8c1.

The present reconstructed density (containing information to 34 Å from 29 particles) can be compared with that of the FMDV C-S8c1/SD6-Fab complex (containing information to 30 Å from 30 particles), where the Fab occupancy is 100% and the Fab has a very well-defined position (Figs. 2 and 3). FMDV C-S8c1 has a remarkably smooth surface at low resolution and, in the FMDV C-S8c1/4C4-Fab reconstruction, there is insufficient surface detail to allow unambiguous determination of the hand of the reconstructed complex.

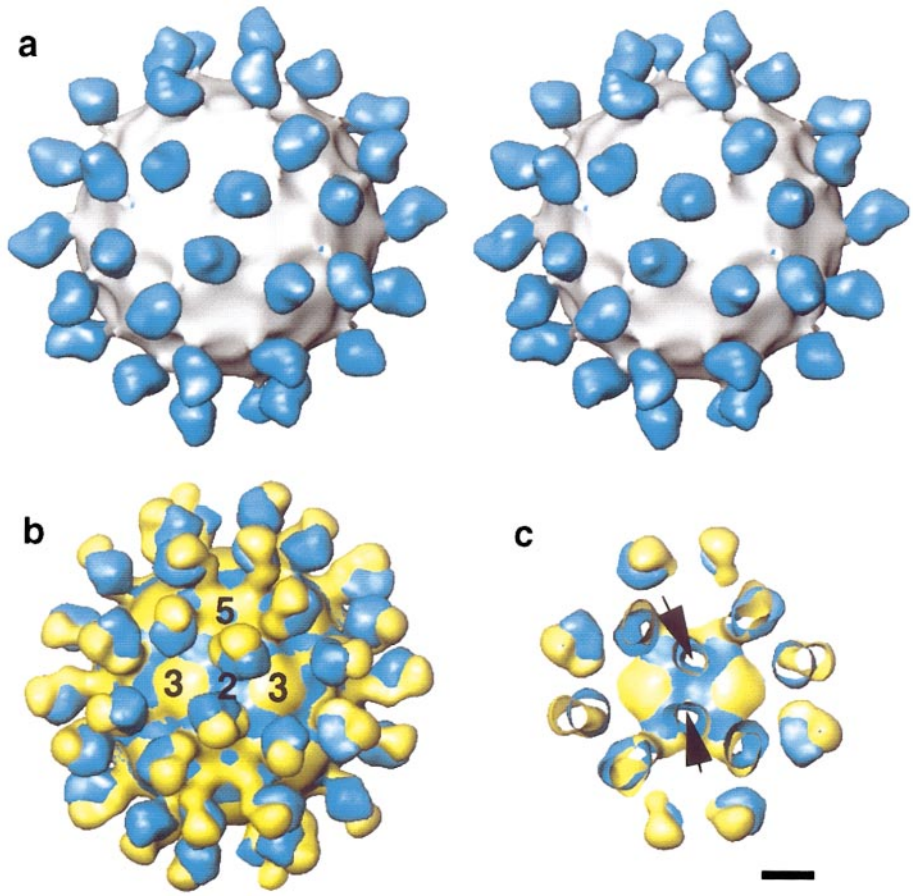

FIG. 2. (a) Stereo view of the isosurface representation of the reconstructed FMDV C-S8c1/4C4-Fab complex. The 4C4-Fab is coloured in blue (R > 150 Å), and the viral capsid (R < 150Å) in gray. (b) Superposition of the reconstructed FMDV C-S8c1/4C4-Fab complex (blue) and the FMDV C-S8c1/SD6-Fab complex (gold) viewed down a twofold axis. (c) A thick section from b (~40-Å-thick parallel to the plane of the page) showing the superimposed footprints of Fabs 4C4 and SD6 (arrows) on the FMDV capsid. All reconstructions are viewed down an icosahedral twofold axis. The scale bar represents 50 Å.

Location of the Fab on the viral surface

The x-ray structure of the 4C4 Fab complexed with the 15-mer peptide, which mimics the VP1 G-H loop of FMDV C-S8c1 (Verdaguer *et al.,* 1998), was initially placed visually in the cryoelectron microscopy density map. The position of contact of the 4C4 Fab on the capsid surface was quite clear, and the long axis of the Fab could be roughly defined. However, the orientation of the Fab about its long axis is not immediately obvious. There are several different orientations of the Fab that appear almost equally probable.

Because the hand of the reconstruction was uncertain, the fitting of the models of virus and 4C4 Fab was done for both enantiomorphs. For one enantiomorph, the fitting was sterically implausible because the Fab-bound G-H loop was displaced from the corresponding loop ends in the capsid structure of FMDV type C (Lea *et al.,* 1994), thus appearing as a sterically unfeasible fitting. Therefore, only modeling in the most probable enantiomorph is presented here. This enantiomorph also showed a higher correlation with the electron density of the three-dimensional reconstruction of the related SD6–FMDV complex for which the hand was determined directly (Hewat *et al.,* 1997) (Figs. 2 and 4).

The rigid body fitting within the electron microscopy density of the x-ray structure of the 4C4 Fab is very sensitive to both lateral and radial displacements and to the angle formed by the longest Fab axis with respect to the viral surface (Table 1). However, even refinement did not allow a clear discrimination between the several orientations that correspond to different rotations around one of the Fab pseudo-twofold axis (Table 1). The orientation defined by a rotation of ~270 degrees, with respect to the orientation of the Fab in the SD6 complex model (Hewat *et al.,* 1997), gives the best agreement factors with a 0.5 occupancy of the Fab (Table 1). Docking in this orientation facilitates modeling of the connection of the ends of the Fab bound peptide with the ordered base of the VP1 G-H loop in the viral structure (Fig. 4). It is not surprising that the orientation with the second best agreement factor is at 90 degrees (i.e., 180 degrees rotation about the pseudo-twofold axis from the

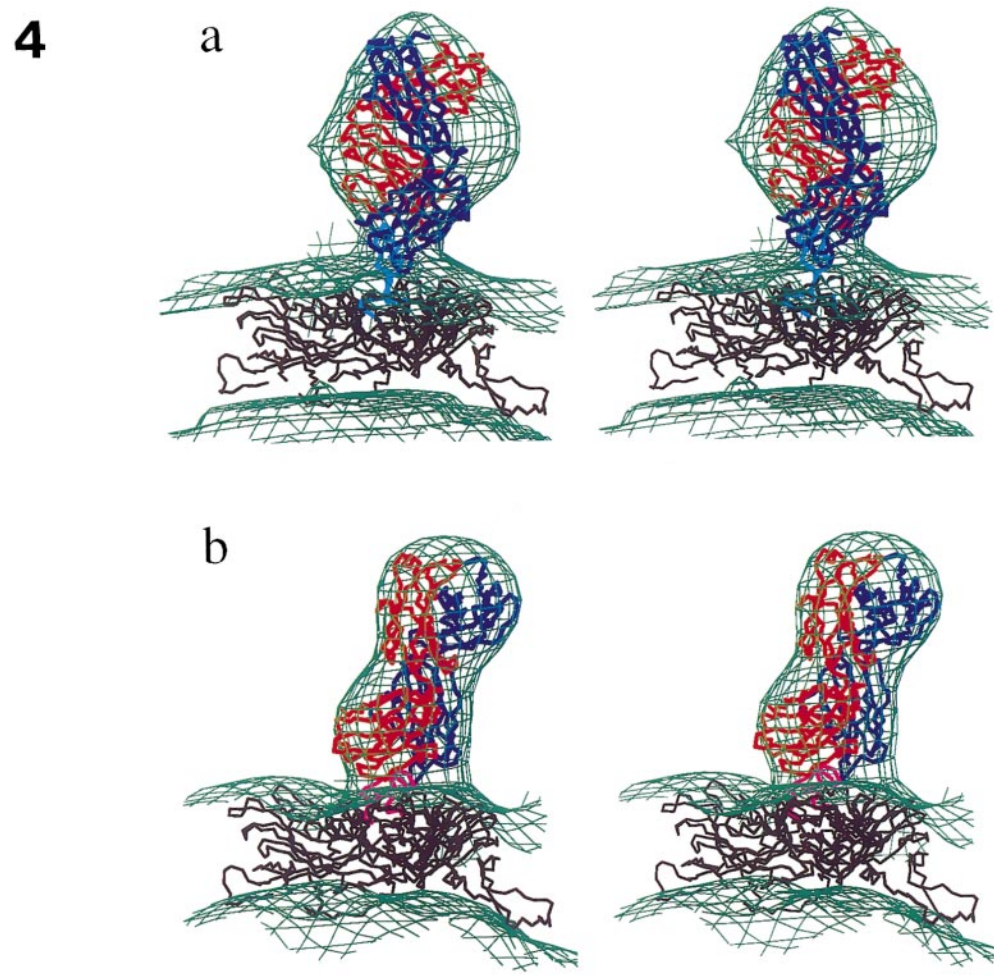

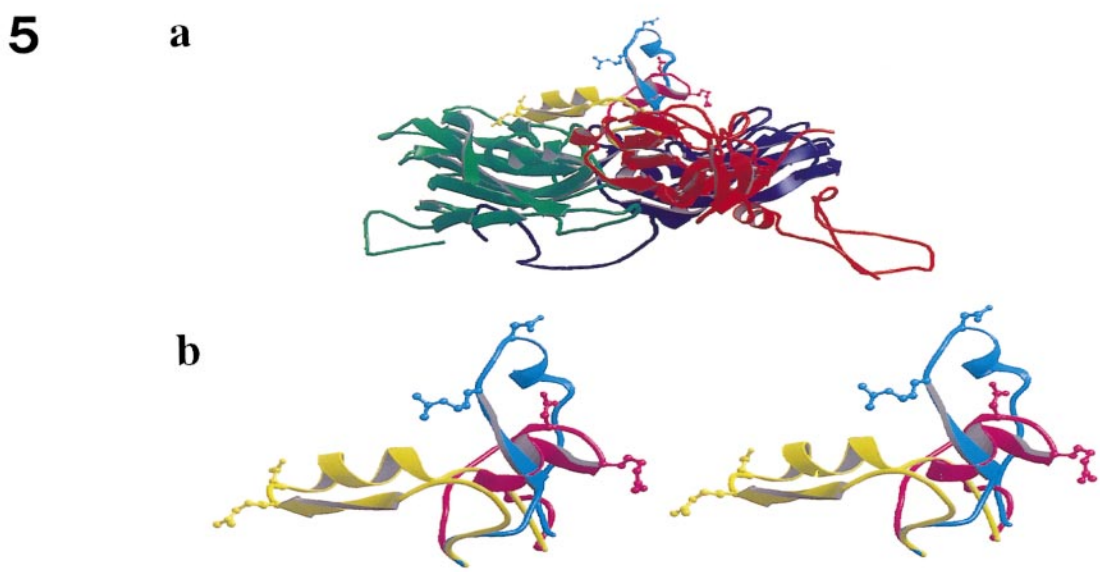

FIG. 4. Stereo views of the complexes between FMDV C-S8c1 and the Fabs 4C4 (a) and SD6 (b). The cryoelectron microscopy map is represented in green. The Cα tracing of the Fab fragments are indicated in red and blue for the heavy and light chains, respectively. All viral proteins are shown in black. The peptides corresponding to the G-H loops are represented in cyan and magenta in a and b, respectively. The different orientations found for the two site A-specific Fabs imply a different location of the G-H loop in these complexes.

FIG. 5. (a) Ribbon diagram of the viral proteins VP1 (blue), VP2 (green), and VP3 (red). The VP1 G-H peptide derived from the reconstructed model is shown in cyan. For comparison, the disposition of the G-H loop determined in the cryoelectron microscope complex between FMDV and the Fab SD6 is shown in magenta, and the location of the loop determined in the crystallographic structure of the reduced FMDV-O1 BFS is indicated in yellow. (b) Enlarged stereo view of the relative disposition of the VP1 G-H loops. The side chains of arginine and aspartic acid from the essential RGD are shown explicitly.

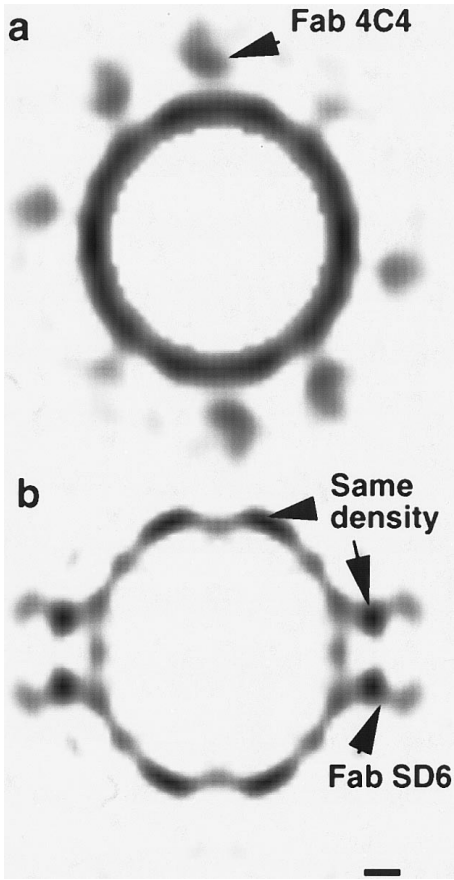

FIG. 3. Sections through the reconstructed density maps of the FMDV C-S8c1/4C4-Fab complex (a) and the FMDV C-S8c1/SD6-Fab complex (b). The sections are chosen to pass through the maximum Fab density. The section in b passes through the origin, and the maximum density in the capsid and in the SD6-Fab are the same (arrows). The section in a is parallel to that in b but at a distance of 25 Å. The maximum density in the 4C4-Fab is 60% of the maximum density in the capsid. The scale bar represents 50 Å.

best orientation). The alternative orientations may reflect the continued flexibility of the "hinge regions" of the G-H loop even when the 4C4 Fab is bound. As indicated previously, the large volume and the relatively weak values of the density corresponding to the Fab fragments also suggest the simultaneous presence of a number of Fab positions.

Geometry of the 4C4 binding

For the proposed model, the shortest distance between the C-terminal ends of the Fab heavy chains is 84 Å. This distance corresponds to the Fab fragments related by the icosahedral twofold axis. The epitopes related by the viral dyad axis are separated by 70 Å. When different Fab orientations are considered, distances between Fab fragments range from 60 to 95 Å. All of these distances are too large to allow two Fab fragments to be linked together on the same viral particle; thus only monovalent binding of the MAb 4C4 to the viral surface seems feasible. This is also supported by studies on neutralisation of infectivity (see below). The only direct interactions between the 4C4 Fab fragments and the viral capsid appear to involve residues from the G-H loop.

G-H loop position

The GH-loop in native FMDV-C is apparently mobile, and most of the loop residues were missing in the crystallographic coordinates of the type C FMDV (Lea *et al.,* 1994). Therefore, the location of the loop in the complex was defined only by the best-fit position of the Fab 4C4 onto the viral shell (Fig. 4). In the proposed model, the G-H loop is located in a fully exposed position clearly different than that found for the loop when interacting with antibody SD6 (Hewat *et al.,* 1997) (Fig 5). The loop is extended so the RGD motif lies at its maximal distance from the capsid surface. The location of the G-H loop also differs from the disposition of the equivalent loop in reduced FMDV type O (Logan *et al.,* 1993) (Fig. 5). However, a simple hinge rotation at the surface of the capsid would allow the transition between the loop position in reduced FMDV type O and when bound to the Fab 4C4. When the Fab SD6 is bound, the loop is also in an "up" position, but it is twisted around its base by ~180 degree and so remains closer to the capsid surface. The possibility of large movements of the loop has already been suggested (Parry *et al.,* 1990).

It is notable that for adenovirus serotype 2, it was reported (Stewart *et al.,* 1997) that a neutralising MAb, which binds to an RGD motif on the virus, is also mobile

TABLE 1

Refinement Statistics in the Reciprocal Space Refinement for the FMDV C-S8c1/4C4 Fab Complex

Model orientation[a]	R-work (%)
4C4-0	31.8
4C4-90	29.6
4C4-180	30.0
4C4-225	30.5
4C4-270[b]	29.7
4C4-315	30.0
Reference[c]	40.5

Note. $R = \Sigma_h \| F_{obs}(h) | - k|F_c(h)| / \Sigma h |F_{obs}(h)|$.

[a] The starting orientations of the 4C4 models were obtained by a rotation around one of the Fab twofold axis (see text). The orientation of the SD6 model was used as the reference orientation (0° rotation). For each model, the initial positioning of the Fab fragments inside the density was chosen manually and refined by rigid body fitting using XPLOR.

[b] Orientation used to represent the 4C4 docking in the figures presented in this work.

[c] The refinement of the 4C4 docking starting with the position of the SD6 model was used as an unbiased reference.

when bound. This RGD motif is believed to be located on a flexible loop and is also the site of interaction for an integrin receptor.

Structural comparison between the two site A-specific antibodies: 4C4 and SD6

The location and disposition of electron density corresponding to the Fab fragments appear to be similar in three-dimensional reconstructions of both the 4C4 and SD6 complexes (Hewat *et al.,* 1997). However, based on the proposed models, the 4C4 Fab fragments seem to interact exclusively with residues from the G-H loop, whereas the Fab SD6 fragments could also present a small number of specific interactions with other capsid regions. The absence of such additional specific interactions outside the loop might explain the larger mobility of the 4C4 Fab moiety when bound to the virion surface. In the x-ray structure of the Fab SD6 cocrystallised with the 15-mer peptide that mimics the VP1 epitope, all 15 peptide residues are resolved and the Fab SD6 interacts closely with 10 of these residues. However, in the x-ray structure of the complex of the Fab 4C4 with the 15-mer peptide, only 10 residues of the peptide are resolved, and the Fab 4C4 interacts closely with 8 of these residues. The 10 common peptide residues, resolved in both of these complexes, which include the RGD motif, have essentially the same conformation. (Verdaguer *et al.,* 1998).

Mechanism of neutralisation by antibodies directed to site A

The neutralisation profile of FMDV C-S8c1 by MAb 4C4 indicates a reduction of 90% of infectivity over an antibody-to-virus input ratio of ~60 (Fig. 6a). The MAb could achieve a million-fold reduction in viral infectivity. No substantial fraction of residual infectivity or U-shaped neutralisation curve (indicative of a weak neutraliser or aggregating antibody, respectively) was found. MAb 4C4 thus is an efficient neutraliser with very similar neutralising characteristics to MAb SD6 (Verdaguer *et al.,* 1997).

To test whether bivalence was required to neutralise infectivity, the neutralisation activity of the purified monovalent Fab was compared with that of the purified Fab2 and the intact MAb and no significant differences were found (Fig. 6b). On a molar basis, the neutralisation activity of MAb or Fab2 was at most sixfold larger than that of Fab (it must be considered that each MAb or Fab2 molecule has two potential attachment sites to the virus, whereas Fab has only one). The similarity of the neutralisation curves strongly supports monovalent binding of the MAb 4C4 to the FMDV capsid. Similar behaviour was also observed in the neutralisation experiments with MAb SD6 (Verdaguer *et al.,* 1997). Both antibodies neutralise the FMDV infectivity with an almost identical efficiency by monovalent antibody binding. Also, both antibodies interact with the peptide epitope in a similar fashion, as deduced from the crystallographic structure in the complexes (Verdaguer *et al.,* 1995, 1998), making direct contact with the integrin receptor recognition triplet RGD. Therefore, despite the larger flexibility of the FMDV C-S8c1/4C4 Fab complex with respect to the SD6 complex and the differences in their interactions with the capsid, we conclude that steric inhibition of the receptor binding site is the major mechanism by which both antibodies neutralise FMDV infectivity and that bivalent binding is not required for FMDV neutralisation. Hinge movements of the FMDV loop may help in accommodating different neutralising antibodies.

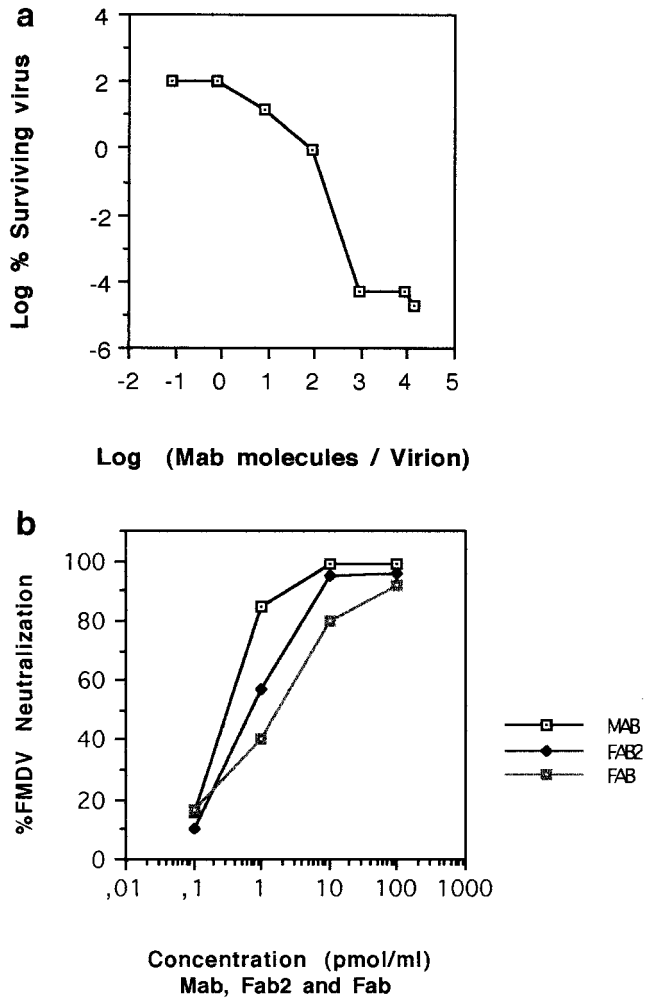

FIG. 6. (a) Neutralisation of FMDV as a function of the antibody 4C4-to-virion input ratio. (b) Neutralisation by antibody 4C4 fragments. The molar amounts of MAb Fab2 and Fab are indicated on the abscissa.

MATERIALS AND METHODS

Preparation of virus and antibody

FMDV C-S8c1 is a biological clone derived from the isolate C1 Sta Pau Sp/70 as previously described (So-

brino *et al.,* 1983). It was purified using the standard procedures described by Curry *et al.* (1992). Site A-specific MAb 4C4 was raised against C1 Brescia It/64 (Capucci *et al.,* 1984) and reacts with both C1 Brescia It/64 and C-S8c1 in enzyme-linked immunosorbent assays, with VP1 in Western blots, and with synthetic peptides representing the antigenic site A of FMDV C-S8c1 (Mateu *et al.,* 1990). The VP1 G-H loop of FMDV C1 Brescia It/64 is identical to that of C-S8c1 except that it has a T instead of an A at position 140 and an A instead of a T at position 149. MAb 4C4 and its Fab fragment were prepared and purified as described by Verdaguer *et al.* (1998).

Preparation of virus-Fab complexes

The type C FMDV and 4C4-Fab complex was prepared and purified as described previously (Hewat and Blaas, 1996, Hewat *et al.,* 1997). FMDV C-S8c1 (33 μg) and 4C4-Fab were incubated at a molar ratio of 1:200 in a volume of 50 μl for 1 h at room temperature. Excess Fab was removed by passage through a Sephacryl S300 spun column (Pharmacia).

Preparation of frozen hydrated specimens

Frozen hydrated specimens were prepared on holey carbon grids as previously described (Hewat *et al.,* 1997). The carbon films, supported on 400 mesh grids, were not ionised before use. Samples of the virus suspension (4 μl) were applied to grids, blotted immediately with filter paper for 1–2 s, and rapidly plunged into liquid ethane cooled by nitrogen gas at −175°C. Specimens were photographed at a temperature of close to −180°C using a Gatan single-tilt cryoholder in a Jeol 1200 EX instrument operating at 100 kV. Images were obtained under low-dose conditions (<20 e/Å^2) at a nominal magnification of 30,000× at ~1.8 and ~3.0 μm underfocus. All the experimental work involving FMDV C-S8c1, including use of the electron microscopy, was performed under P3 laboratory conditions at The Institute for Animal Health, Pirbright.

Image analysis

Preliminary selection of micrographs, digitisation, and preparation of virus particle images for analysis were performed as described previously (Hewat *et al.,* 1992). The pixel size of 20.9 μm on the micrograph corresponds to a pixel size of 6.75 Å/pixel at the specimen. Further image analysis was performed on a DEC Alpha workstation using modified versions of the MRC icosahedral programs and the polar Fourier transform, PFT, model-based orientation determination programs (Baker and Cheng, 1996) supplied by S. Fuller (Fuller *et al.,* 1996). The particle orientations and origins were determined using the PFT model based approach, using a starting model derived from the reconstruction of the FMDV-C-S8c1/SD6-Fab complex. The starting model consisted of the FMDV capsid and a small portion of the variable region of the SD6 Fab (i.e., the reconstruction was truncated below a radius of 98 Å and beyond 160 Å). The resulting reconstruction of the FMDV-C-S8c1/4C4-Fab complex was then similarly truncated and used as a model for the next cycle of refinement. The closer to focus images were refined through numerous cycles. Only particles with a cross-correlation coefficient of >0.40 were retained. The best reconstruction used 29 particles and included information to 34-Å resolution. Isosurface representations of the reconstructed density were visualised using EXPLORER, and the density maps were visualised using SEMPER 6 Plus on a Silicon Graphics workstation.

The relatively poor quality of this reconstruction and the lack of surface detail on the virus capsid arise from the extreme difficulty in determining the orientations of the images of the complex where a significant part of the density is not related by icosahedral symmetry, arising from the Fab mobility and/or partial occupancy, and an almost spherical virus. By comparison, in the case of the complex between human rhinovirus serotype 2 and the Fab 3B10, the 80% occupancy of the Fab did not substantially hinder the icosahedral 3D reconstruction (Hewat *et al.,* 1998). Also, in the case of a calicivirus with 50% MAb occupancy, the icosahedral 3D reconstruction was not so difficult because the arched capsomers on the capsid conferred a much higher icosahedral content on the complex (Thouvenin *et al.,* 1997). In both of these cases, the Fabs had a well-defined position indicating little or no Fab movement.

Fitting the FMDV C-S8c1 and 4C4-Fab x-rays structures to the cryoelectron microscopy density

The magnification of the electron microscopically reconstructed density map of the complex was determined by scaling it to the x-ray data as described by Hewat *et al.* (1997). The reconstructed map was then masked to exclude all density except that corresponding to the capsid and the Fab. This was done by subtracting the mean density from the reconstructed map and setting all density below zero to zero. The density at a radius below 110 Å (corresponding to the viral RNA) was also set to zero. No correction was made for the electron microscope contrast transfer function.

The x-ray structure of the Fab 4C4 was first fitted by eye to the cryoelectron microscope density map using the program O (Jones *et al.,* 1991). The large volume of the Fab density defines the Fab pseudo-twofold axis reasonably well but does not allow determination of the rotation angle of the Fab about this axis. To determine the best fit, the structure factors corresponding to the electron microscope density of the Fab–virus complex were calculated by Fourier transformation and used to

refine the structures with the program XPLOR (Brünger 1993) by rigid-body minimisation at 35 Å resolution. Strict icosahedral symmetry was always imposed with the appropriate 60 noncrystallographic symmetry operators, and the model of the viral shell was kept fixed. The temperature factors for both capsid and Fab were set to 2000 $Å^2$. Refinement of the Fab molecule, always treated as a single rigid body, was evaluated using the R-factor (Table 1).

G-H loop modeling

The VP1 G-H loop was assumed to adopt essentially the conformation found for the 15-mer peptide complexed with the 4C4 Fab in the crystallographic structure, where only 10 of the 15 residues were clearly visible in the electron density maps (Verdaguer *et al.,* 1998). The location of the peptide with respect to the viral surface was defined by positioning of the Fab during the rigid body refinement. Modeling was thus limited to linking the N and C peptide ends to the known structure of VP1 (Lea *et al.,* 1994). Four residues (T133, T134, A135, and Y136) at the N-terminal portion of the peptide and five residues (T148, T149, T150, H151, and A152) at the C-terminus were missing from the FMDV type C structure. These residues were manually introduced using the graphic program TURBO (Rousel and Cambillau, 1991). The direct link of the two peptide ends to the virus required only minor rearrangements.

Neutralisation experiments

The neutralisation profile of FMDV C-S8c1 by MAb 4C4 was measured as follows. A total of 4.5×10^7 PFU (4.5×10^{11} virions) was mixed with different amounts of purified MAb 4C4, the mixtures were incubated for 1 h at room temperature, and infectivity was determined in a plaque reduction assay as previously described (Mateu *et al.,* 1987). The ratio of physical-to-infectious particles for FMDV C-S8c1 in purified FMDV preparations were determined by evaluating the virus titers in infectivity assays and by measuring the amounts of viral proteins by SDS–PAGE and densitometry. This ratio was ~10,000 virions/PFU. The comparison of the neutralisation activity by the antibody 4C4 and its fragments was done by plaque reduction neutralisation assays (Mateu *et al.,* 1987) using equimolar amounts of MAb, Fab, and Fab2.

ACKNOWLEDGMENTS

We thank S. Fuller for supplying his versions of the MRC icosahedral programs, J. Newman for maintaining the electron microscope, W. Blakemore for preparing the FMDV C, E. Brocchi for the supply of MAb 4C4 and for a very helpful collaboration, and R. H. Wade for support. This work was funded in part by the DGICYT (Grants PB95–0218 and PB94–0034-C02–01), MAFF, and Fundación Ramón Areces. N.V. thanks the EMBO for fellowships ASTF8089 and ASTF8375.

REFERENCES

Acharya, R., Fry, E., Stuart, D., Fox, G., Rowlands, D., and Brown, F. (1989) The three dimensional structure of foot-and-mouth disease virus at 2.8 Å resolution. *Nature* **337**, 709–716.

Baker, T. S., and Cheng, R. H. (1996). A model based approach for determining orientations of biological macromolecules imaged by cryoelectron microscopy. *J. Struct. Biol*. **116,** 120–130.

Berinstein, A., Roivainen, M., Hovi, T., Mason, P. W., and Baxt, B. (1995). Antibodies to the vitronectin receptor (integrin $\alpha_v\beta_3$) inhibit binding and infection of foot-and-mouth disease virus to cultured cells. *J. Virol*. **69,** 2664–2666.

Bittle, J. L., Houghten, R. A., Alexander, H., Shinnick, T. M., Sutcliffe, J. G., Lenner, R. A., Rowlands, D. J., and Brown, F. (1982). Protection against foot-and-mouth disease virus by immunization with a chemically synthesized peptide predicted from the viral nucleotide sequence. *Nature* **298,** 30–33.

Brünger, A. T. (1993). "XPLOR Manual, Version 3.1." Yale University, New Haven, CT.

Capucci, L., Brocchi, E., De Simone, F., and Panini, G. F. (1984). Characterisation of monoclonal antibodies against foot-and-mouth disease virus. In "Report of a Session of the Research Group of the Standing Technical Committee of the European Commission for the Control of Foot-and-Mouth Disease. Food and Agriculture Organization," United Nations, Brescia, Italy, pp. 32–39.

Curry, S., Abu-Ghazaleh, R., Blakemore, W., Fry, E., Jackson, T., King, A., Lea, S., Logan, D., Newman, J., and Stuart, D. (1992). Crystallisation and preliminary X-ray analysis of three serotypes of foot-and-mouth disease virus. *J. Mol. Biol*. **228,** 1263–1268.

Curry, S., Fry, E., Blackmore, W., Abu-Ghazaleh, R., Jackson, T., King, A., Lea, S., Newman, J., Rowlands, D., and Stuart, D. (1996). Perturbations in the surface structure of A22 Iraq foot-and-mouth disease virus accompanying coupled changes in host cell specificity and antigenicity. *Structure* **4,** 135–145.

DiMarchi, R., Brooke, G., Gale, C., Cracknell, V., Doel, T., and Mowat, N. (1986). Protection of cattle against foot-and-mouth disease virus by synthetic peptide. *Science* **232,** 639–641.

Domingo, E., Escarmis, C., Martines, M. A., Martinez-Salas, E., and Mateu, M. G. (1992). Foot-and-mouth disease virus populations are quasispecies. *Curr. Topics Microbiol. Immunol.* **176,** 33–47.

Fox, G., Parry, N., Barnett, P. V., McGinn, B., Rowlands, D. J., and Brown, F. (1989). The cell attachment site on foot-and-mouth disease virus includes the amino acid sequence RGD (arginine-glycine-aspartic acid). *J. Gen. Virol*. **70,** 625–637.

Fuller, S. D., Butcher, S. J., Cheng, R. H., and Baker, T. S. (1996). Three-dimensional reconstruction of icosahedral particles: The uncommon line. *J. Struct. Biol*. **116,** 48–55.

Hernandez, J., Valero, M., Andreu, D., Domingo, D., and Mateu, M. G. (1996). Antibody and host cell recognition of foot-and-mouth disease virus (serotype C) cleaved at the Arg-Gly-Asp motif: A structural interpretation. *J. Gen. Virol*. **77,** 257–265.

Hewat, E. A., and Blaas, D. (1996). Structure of a neutralizing antibody bound bivalently to human rhinovirus 2. *EMBO J*. **15,** 1515–1523.

Hewat, E. A., Booth, T. F., Loudon, P. T., and Roy, P. (1992). Three-dimensional reconstruction of baculovirus expressed bluetongue virus core-like particles by cryoelectron microscopy. *Virology* **189,** 10–20.

Hewat, E. A., Marlovitz T., and Blaas, D. (1998). Structure of a neutralizing antibody bound monovalently to human rhinovirus 2. *J. Virol*. **72,** 4396–4402.

Hewat, E. A., Verdaguer, N., Fita, I., Blakemore, W., Brookes, S., King, A., Newman, J., Domingo, E., Mateu, M. G., and Stuart, D. (1997). Structure of the complex of an Fab fragment of a neutralizing antibody with foot-and-mouth disease virus: Positioning of a highly mobile antigenic loop. *EMBO J*. **16,** 1492–1500.

Jackson, T., Sharma, A., Ghazaleh, R. A., Blakemore, W. E., Ellard, F. M., Simmons, D. L., Newman, J. W., Stuart, D. I., and King, A. M. (1997). Arginine-glycine-aspartic acid-specific binding by foot-and-mouth

disease viruses to the purified integrin alpha(v)beta3 in vitro. *J. Virol*. **71,** 8357–8361.

Jones, T. A., Zou, Y. J., Cowan, S. W., and Kjeldgaard, M. (1991). Improved methods for building protein models in electron density maps and the location of errors in these models. *Acta Crystallogr. A* **47,** 110–119.

Lea, S., Abu-Ghazaleh, R., Blakemore, W., Curry, S., Fry, E., Jackson, T., King, A., Logan, D., Newman, J., and Stuart, D. (1995). Structural comparison of two strains of foot-and-mouth disease virus subtype O_1 and a laboratory antigenic variant, G67. *Structure* **3,** 571–580.

Lea, S., Hernández, J., Blakemore, W., Brocchi, E., Curry, S., Domingo, E., Fry, E., Abu-Ghazaleh, R., King, A., Newman, J., Stuart, D., and Mateu, M. G. (1994). The structure and antigenicity of serotype C foot-and-mouth disease virus. *Structure* **2,** 123–139.

Logan, D., Abu-Ghazaleh, R., Blakemore, W., Curry, S., Jackson, T., King, A., Lea, S., Lewis, R., Newman, J., Parry, N., Rowlands, D., Stuart, D., and Fry, E. (1993). Structure of a major immunogenic site on foot-and-mouth disease virus. *Nature* **362,** 566–568.

Mason, P. W., Rieder, E., and Baxt, B. (1994). RGD sequence of foot-and-mouth disease virus is essential for infecting cells via the natural receptor but can be bypassed an antibody-dependent enhancement pathway. *Proc. Natl. Acad. Sci. USA* **91,** 1932–1936.

Mateu, M. G. (1995). Antibody recognition of picornaviruses and escape from neutralization: A structural view. *Virus Res.* **38,** 1–24.

Mateu, M. G., Andreu, D., Carreno, C., Roig, X., Cairo, J. J., Camarero, J. A., Giralt, E., and Domingo E. (1992). Non-additive effects of multiple amino acid substitutions on antigen-antibody recognition. *Eur. J. Immunol*. **22,** 1385–1389.

Mateu, M. G., Martinez, M. A., Capucci, L., Andreu, D., Giralt, E., Sobrino, F., Brocchi, E., and Domingo, E. (1990). A single aminoacid substitution affects multiple overlapping epitopes in the major antigenic site of foot-and-mouth disease virus of serotype C. *J. Gen. Virol*. **71,** 629–637.

Mateu, M. G., Rocha, E., Vicente, O., Vayreda, F., Navalpotro, C., Pedroso, E., Enjuanes, L., Giralt, E., and Domingo, E. (1987). Reactivity with monoclonal antibodies of viruses from an episode of foot-and-mouth disease. *Virus Res.* **8,** 261–274.

McCullough, K. C., De Simone, F., Brocchi, E., Capucci, L., Crowther, J. R., and Kihm, U. (1992). Protective immune response against foot-and-mouth disease. *J. Virol*. **66,** 1835–1840.

Parry, N., Fox. G., Rowlands, D., Brown, F., Fry, E., Acharya, R., Logan, D., and Stuart, D. (1990). Structural and serological evidence for a novel mechanism of antigenic variation in foot-and-mouth disease virus. *Nature* **347,** 569–572.

Pfaff, E., Mussgay, M., Bohm, H. O., Schultz, G. E., and Shaller, H. (1982). Antibodies against a preselected peptide recognize and neutralize foot-and-mouth disease virus. *EMBO J.* **1,** 869–874.

Rousel, A., and Cambillau, C. (1991). TURBO. In "Silicon Graphics Directory." Mountain View, CA.

Rueckert, R. R. (1996). Picornaviridae: The viruses and their replication. In "Fields' Virology"(B. N. Fields, et al., eds.), pp. 609–654, Lippincott-Raven Publishers, Philadelphia.

Sharma, A., Rao., Z., Fry, E., Booth T., Jones, E. Y., Rowlands, D. J., Simmonds, D. L., and Stuart, D. I. (1996). Specific interactions between human integrin $\alpha_v\beta_3$ and chimeric hepatitis B virus core particles bearing the receptor binding epitope of foot-and-mouth disease virus. *Virology* **239,** 150–157.

Sobrino, F., Dávila, M., Ortin, J., and Domingo, E. (1983). Multiple genetic variants arise in the course of replication of foot-and-mouth disease virus in cell culture. *Virology* **128,** 310–318.

Stewart, P. L., Chiu, C. Y., Huang, S., Muir, T., Zhao, Y., Chait, B., Mathias, P., and Nemerow, G. R. (1997). Cryo-EM visualization of an exposed RGD epitope on adenovirus that escapes antibody neutralization. *EMBO J*. **16,** 1189–1198.

Taboga, O., Tami, C., Carrillo, E., Nuñez, J. I., Rodriguez, J., Saiz, J. C., Blanco, E., Valero, M.-L., Roig, X., Camarero, J. A., Andreu, D., Mateu, M. G., Giralt, E., Domingo, E., Sobrino, F., and Palma, E. L. (1997). A large scale evaluation of peptide vaccines against foot-and-mouth disease: Lack of solid protection in cattle and isolation of escape mutants. *J. Virol*. **71,** 2606–2614.

Thouvenin, E., Laurent, S., Madelaine, M-F., Rasschaert, D., Vautherot, J.-F., and Hewat, E. A. (1997). Bivalent binding of a neutralising antibody to a calicivirus involves the torsional flexibility of the antibody hinge. *J. Mol. Biol*. **270,** 238–246.

Verdaguer, N., Fita, I., Domingo, E., and Mateu, M. G. (1997). Efficient neutralization of foot-and-mouth disease virus by monovalent antibody binding. *J. Virol.* **71,** 9813–9816.

Verdaguer, N., Mateu, M. G., Andreu, D., Giralt, E., Domingo, E., and Fita, I. (1995). Structure of the major antigenic loop of foot-and-mouth disease virus complexed to anti-virus neutralizing antibody. Direct involvement of Arg-Gly-Asp in the interaction. *EMBO J.* **14,** 1690–1696.

Verdaguer, N., Mateu, M. G., Bravo, J., Domingo, E., and Fita, I. (1996). Induced pocket to accommodate the cell attachment Arg-Gly-Asp motif to a neutralizing antibody against foot-and-mouth disease virus. *J. Mol. Biol*. **256,** 364–376.

Verdaguer, N., Sevilla, N., Valero, M., Stuart, D., Brocchi, E., Andreu, D., Giralt, E., Domingo, E., Mateu, M. G., and Fita, I. (1998). A similar pattern of interaction for different antibodies with a major antigenic site of foot-and-mouth disease virus: Implications for intratypic antigenic variation. *J. Virol*. **72,** 739–748.